American Mineralogist, Volume 64, pages 288–293, 1979

Free energies of decarbonation reactions at mantle pressures: I. Stability of the assemblage forsterite–enstatite–magnesite in the system $MgO–SiO_2–CO_2–H_2O$ to 60 kbar

DAVID H. EGGLER[1], IKUO KUSHIRO[2]

Geophysical Laboratory, Carnegie Institution of Washington
Washington, D.C. 20008

AND JOHN R. HOLLOWAY

Department of Chemistry, Arizona State University
Tempe, Arizona 85281

Abstract

The stability of the assemblage forsterite–enstatite–magnesite in the presence of $CO_2–H_2O$ vapor, limited by the reaction $MgSiO_3 + MgCO_3 = Mg_2SiO_4 + CO_2$, has been determined at 26 kbar pressure. Activity coefficients for CO_2 calculated from experimental data (1.40 ± 0.15 at $XCO_2 = 0.5$ and 1.62 ± 0.13 at $XCO_2 = 0.3$) are sufficiently close to values predicted by modified Redlich-Kwong (MRK) functions (Holloway, 1977) to warrant calculation of the divariant decarbonation surface to 60 kbar.

The calculations are possible because of a reliable set of 1-bar free energies for the above reaction in the absence of H_2O. Experimental brackets on the reaction from Newton and Sharp (1975) at 19–41 kbar, from Johannes (1969) at 2 kbar, and from new runs at 26 and 30 kbar were reduced to 1-bar free energies using MRK CO_2 fugacities. All experimental brackets are consistent with the equation $\Delta G^0_{T,1\,bar} = 21{,}337 - 41.05T(°K) \pm 400$ cal.

From the new calculations it appears that carbonates (magnesite and dolomite) are stable phases in peridotite assemblages in the mantle, even in the presence of very H_2O-rich vapor.

Introduction

The importance of carbonate minerals in the mantle has been realized in the past several years. Carbonate minerals may be stable in peridotite mineral assemblages (Newton and Sharp, 1975; Kushiro *et al.*, 1975; Huang and Wyllie, 1975a; Eggler, 1975) and may be participants in the melting of peridotite at high pressures (Wyllie and Huang, 1976; Eggler, 1976).

Decarbonation reactions in the systems $MgO–SiO_2–CO_2$ and $CaO–MgO–SiO_2–CO_2$ at pressures of the mantle have been identified, and many of them have been experimentally investigated (Eggler *et al.*, 1976; Wyllie and Huang, 1976), but the effect of H_2O upon these reactions has not been quantified. For this initial study of the effect of H_2O, a petrologically important decarbonation reaction in the relatively simple system $MgO–SiO_2–CO_2–H_2O$ was selected for investigation by experimental and thermodynamic methods.

Methods

Starting materials

Two starting materials of forsterite (Mg_2SiO_4) composition were used. One was crystalline forsterite. The other was a finely-ground mechanical mixture of SiO_2 (cristobalite), MgO, and natural magnesite ($MgCO_3$), in mole proportions 2 MgO:1 SiO_2:2 CO_2. Weighed amounts of the mechanical mixture or of crystalline forsterite and $Ag_2C_2O_4$, with and without H_2O, were sealed in Pt capsules, placed in 1.27-cm furnace assemblies, and run in solid-media, high-pressure apparatus.

---

[1] Present address: Department of Geosciences, The Pennsylvania State University, University Park, Pennsylvania 16802.

[2] Present address: Geological Institute, University of Tokyo, Hongo, Tokyo 113, Japan.

0003–004X/79/0304–0288$02.00

Duration of runs

Anhydrous experiments were run for 65–200 minutes, whereas hydrous experiments, at somewhat lower temperatures, were run for 240–330 minutes. No discrepancies were noted between experiments run for relatively short *vs.* relatively long times.

Comparison of apparent pressure and of hydration in two assemblies

We found that the reaction

$$MgSiO_3 + MgCO_3 = Mg_2SiO_4 + CO_2 \qquad (1)$$

occurs over a temperature interval, presumably because some H_2O was present in allegedly dry capsules. The H_2O was probably introduced either by adsorption on grain boundaries before the capsules were sealed, or by reaction during the run between CO_2 and H_2 that diffused through the capsule wall. The amount of this H_2, produced by reaction between H_2O from dehydrating talc with graphite and boron nitride, is very small, resulting in a mole fraction $CO_2/(CO_2 + H_2O)$ inside the capsule of only 0.98 (Eggler *et al.,* 1974). Nevertheless, it seemed advisable to make runs also in talc–Pyrex assemblies (Hariya and Kennedy, 1968), which were adopted at the Geophysical Laboratory to prevent access of H_2O to the graphite and sample. This test, in turn, necessitated a comparison of the apparent pressure in talc–BN and talc–Pyrex assemblies, in the light of the results of Huang and Wyllie (1975b), which indicated the need for a significant (10 percent) pressure correction for a Pyrex assembly.

For the tests, 8 mg portions of the mechanical mixture were placed in Pt capsules and dried at 110°C. The capsules were then welded shut. Experiments were conducted in a pressure plate with a new carbide core, using lengths of Pt and Pt10Rh thermocouple wire from the same spools. Runs were 70–90 minutes long, sufficient time for complete reaction to occur (Newton and Sharp, 1975). Runs with talc–Pyrex assemblies were taken to a pressure greater than the nominal pressure and heated to run temperature. The piston was then backed off to the nominal pressure (hot piston-out). Runs in BN assemblies were performed piston-out and floating-piston (piston neither advanced nor retracted during or after heating). The new determinations at 26 kbar are shown in Figure 1.

Hydration of the sample occurred in both Pyrex and BN assemblies, as seen by the development of a Fo + En + Mag + V field between the Fo + V and En + Mag + V fields. The lower temperature boundary of the Fo + En + Mag + V field (with En + Mag + V) lies 25°–35°C below the upper boundary (with Fo + V); part of that apparent temperature interval may be accounted for by temperature gradients along sample capsules. It would appear that Pyrex assemblies are no more effective than BN assemblies in preventing diffusion of H_2 into capsules.

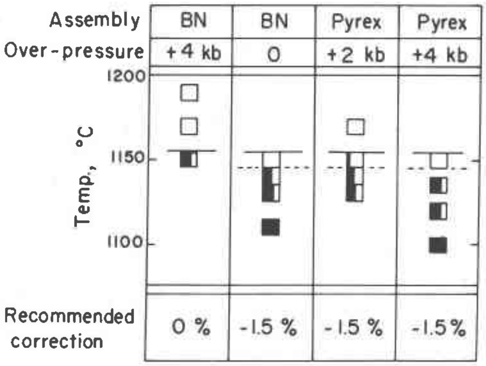

Fig. 1. Results of quenching runs on the reaction $MgSiO_3 + MgCO_3 = Mg_2SiO_4 + CO_2$ at 26 kbar nominal pressure, using two assemblies and several techniques. For each run, the area of the uncertainty box that is shaded represents the estimated amount of enstatite + magnesite present. The solid horizontal line represents the phase boundary between Fo + V and En + Mag + Fo + V that has been determined by thermodynamic smoothing of data of this report (Fig. 2A) and of Newton and Sharp (1975); the dashed lines represent the experimentally-determined boundaries for each set of experiments.

In spite of hydration, the runs can be used to estimate corrections in pressure for different techniques. As will be apparent from later discussion, the upper boundary of the Fo + En + Mag + V field lies less than 5°C below the anhydrous decarbonation curve, for $CO_2/(CO_2 + H_2O) > 0.95$. Because the capsules were at least that dry (Eggler *et al.,* 1974), the upper boundary can be considered to be coincident with the anhydrous decarbonation curve, within experimental uncertainty. The anhydrous decarbonation temperature at 26 kbar, calculated from a smoothed thermodynamic function (see below), is 1155°C. The temperature of decarbonation determined by piston-out runs in BN assemblies is consistent with this temperature, but the temperature of decarbonation determined by other techniques is low by about 10°C (Fig. 1). (The run at 1150°C in Pyrex with a 2 kbar overpressurization contained a minor amount of enstatite + magnesite that was interpreted to have formed by back-reaction upon the quench.) Although it might be argued that a difference of 10°C is within experimental uncertainty, the uncertainty is believed to be less than 10°C *in this case* because of the identical sample-assembly configuration for all

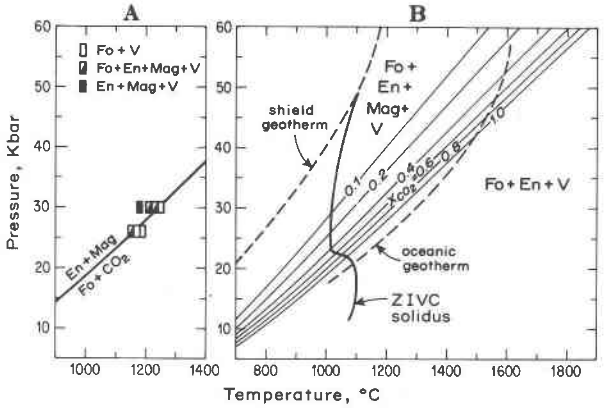

Fig. 2. P–T coordinates of the reaction En + Mag = Fo + CO_2. (A) Runs confirming the position of the anhydrous reaction, using piston-out technique. The boundary shown has been calculated (see text). (B) A family of curves, of equal vapor composition, on the divariant decarbonation surface, denoting the stability limits of the assemblage En + Fo + Mag + vapor (CO_2–H_2O vapor). The curves have been calculated, using MRK thermodynamic functions. The phase assemblages shown are for a peridotite composition in the system MgO–SiO_2–CO_2–H_2O containing less than about 20 weight percent CO_2. Equivalent phase assemblages for natural peridotite compositions are discussed in the text. Also shown are oceanic (Ringwood, 1966) and shield (Clark and Ringwood, 1964) geotherms and a calculated solidus applicable to peridotitic compositions containing amounts of CO_2 and H_2O sufficiently small that the vapor composition is buffered within a zone of invariant composition, a ZIVC (Eggler, 1977).

runs. On this assumption, and because the dT/dP slope of the reaction is 24°C/kbar (Fig. 2A), the pressure of floating-piston runs in BN assemblies should be decreased by 1.5 percent. This correction is probably due to friction. A correction of −1.5 percent should also be applied to piston-out runs with Pyrex assemblies; this correction may reflect a negative anvil effect (Bell and Mao, 1971), resulting from strength differences between strong ceramic pieces and weaker Pyrex and talc pieces.

Thermodynamic calculations

For reaction (1), equilibrium at a particular pressure can be related to a reference state of 1 bar and pure reactants and products by the equation

$$\Delta G_{P,T} = \Delta G_T^0 + \Delta V_s(P - 1) + RT \ln fCO_2 \quad (2)$$

where ΔG_T^0 is the free energy of the reaction at the reference state, P is the pressure in bars, T is the temperature in °K, fCO_2 is the fugacity of CO_2 at P and T, and ΔV_s is the molar volume change of the crystalline phases (assumed to be constant). The fugacity of CO_2 can be expressed, for a given P and T, by the relation

$$fCO_2 = XCO_2 \gamma CO_2 f^0CO_2 \quad (3)$$

where XCO_2 is the mole fraction of CO_2 in the vapor phase, γCO_2 is the CO_2 activity coefficient, and f^0CO_2 is the fugacity of pure CO_2. Values of f^0CO_2 were obtained from the MRK equation of state (Holloway, 1977).

Results

Anhydrous decarbonation

Although reaction (1) has been determined by Newton and Sharp (1975), new runs were made as an interlaboratory comparison (Figs. 1, 2A). As detailed above, the position of the reaction was taken at the upper temperature limit of the assemblage enstatite + magnesite. These new runs and the critical runs of Newton and Sharp (1975) can be reduced to the reference state of 1 bar using equation (2) and MRK CO_2 fugacity coefficients (Fig. 3). Free energies corresponding to P and T at the four corners of the "uncertainty rectangle" for each run, as reported, were calculated and appear as rhombohedra in Figure 3. In the plot of free energies against T, all the runs can be fit with a straight line. In such a plot, constant entropy of reaction is assumed (Zen, 1972).

The equation of the straight line is

$$\Delta G_T^0 = 21{,}337 - 41.05T(°\mathrm{K}) \pm 400 \text{ cal} \quad (4)$$

The uncertainty, estimated from the band of all straight lines fitting the uncertainty rhombohedra,

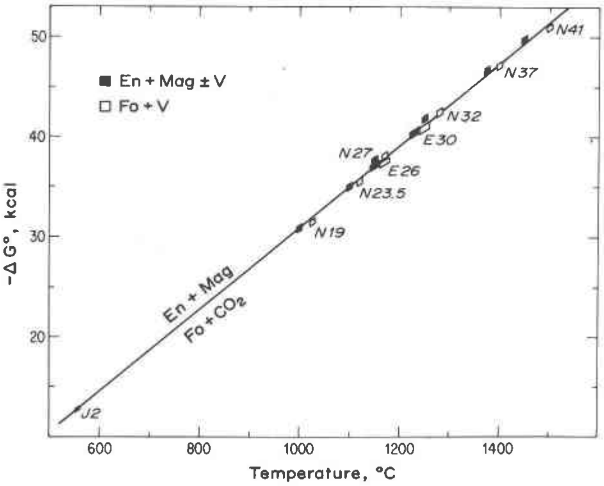

Fig. 3. Free energies of reaction (1) at 1 bar, calculated from bracketing runs of Newton and Sharp (1975) (designated by N, followed by the pressure in kilobars) and of this study (designated by E, followed by the pressure). The lower temperature bracket (J2) encompasses the range of uncertainty in the determination of Johannes (1969) at 2 kbar.

applies to the temperature range 873°-1773°K. The empirical ΔS, 41.05±1.00 cal/°, can be compared with the average ΔS from Robie and Waldbaum (1968) over the temperature range 400°-1100°K (the highest temperature recorded for magnesite), 39.98±1.60. (The entropy of orthoenstatite was taken to be the same as that of clinoenstatite, as recommended by Zen and Chernosky, 1976.)

From the free energy plot (Fig. 3), it is apparent that

(1) The MRK data are internally consistent, inasmuch as data at pressures from 2 to 41 kbar (corresponding to CO_2 fugacities of 3615 to 1.5×10^8 bars) have been reduced to a common line.

(2) There is no significant inconsistency between the data set of Newton and Sharp (1975) and that reported in this paper.

From equations (2) and (4), P–T coordinates of the decarbonation reaction can be calculated. This thermodynamically-smoothed curve appears in Figure 2A.

Hydrous decarbonation

Hydrous runs at 26 kbar delimit the phase field boundary between Fo + V and Fo + En + Mag + V (Fig. 4). For the majority of runs, the mechanical mixture was used; runs in the Fo + En + Mag + V field contained enstatite and discrete grains of magnesite. Runs interpreted to be in the Fo + V field contained traces of intergranular carbonate, probably produced either by solution of silica in the fluid or by back-reaction upon the quench. (Back-reaction is a major problem even in some anhydrous decarbonation reactions [Eggler *et al.*, 1976].) The position of the phase field boundary was checked with one run on a forsterite + $Ag_2C_2O_4$ (Fo + V) starting material (Fig. 4). The boundary has not been reversed, in a strict sense, because a starting material of En + Mag + V was not used. There is no reason to doubt its accuracy, however, given the reactivity of the compositions.

Along the upper curve in Figure 4, the vapor has the $CO_2/(CO_2 + H_2O)$ indicated on the abscissa, because immediately above the upper curve no carbonate is present, and all CO_2 is present in the vapor. Within the field of Fo + En + Mag + V, the composition of vapor, at a given temperature and pressure, is invariant and accordingly can be read in Figure 4 by projecting an isotherm across to the upper curve. (Note, however, that for a point within the Fo + En + Mag + V field, the vapor composition cannot be read directly from the abscissa.) The lower curve in Figure 4 is specific only for the bulk composition studied. Its position can be calculated because the amount of CO_2 tied up in the assemblage En + Mag and (by difference) the amount of CO_2 in the vapor in equilibrium with En + Mag can be determined unambiguously, because vapor compositions within the field of Fo + En + Mag + V can be determined as above, and because the two sets of vapor compositions are equal along a single line in T–X space, namely the lower curve.

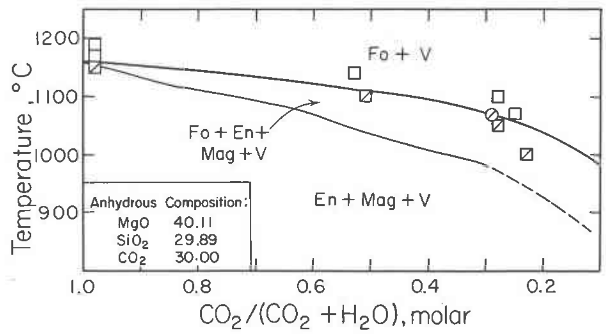

Fig. 4. Results of quenching experiments, using piston-out technique at 26 kbar, on the stability of the assemblage En + Mag + Fo + V (CO_2–H_2O vapor). Along the join studied, various amounts of H_2O were added to the anhydrous composition shown. The abscissa is the mole fraction $CO_2/(CO_2 + H_2O)$ in the bulk composition and denotes vapor composition only within the field of Fo + V. Squares refer to a starting composition of finely-mixed cristobalite, magnesite, and magnesia; circle refers to a composition of forsterite and $Ag_2C_2O_4$. The lower curve is calculated from the upper curve.

The upper curve from Figure 4 is replotted in Figure 5 as a band encompassing the estimated uncertainty in its position, together with the critical runs.

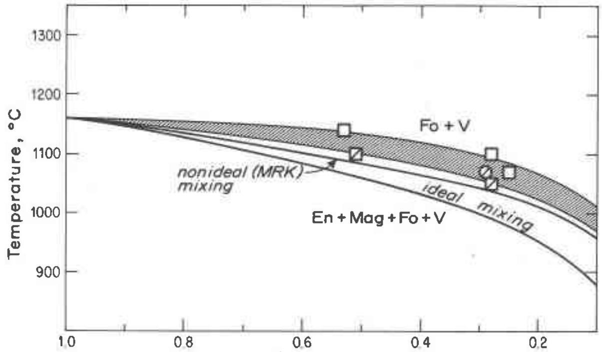

Fig. 5. Comparison of quenching experiments on stability of the assemblage En + Mag + Fo + V at 26 kbar, with decarbonation curves calculated for an ideal mixing model and for nonideal mixing (MRK activity coefficients). The abscissa denotes vapor composition. Symbols are the same as for Fig. 4. The shaded band is the estimated extent of experimental uncertainty.

Also shown in Figure 5 is another set of decarbonation curves calculated using free energies from Figure 3 and equations (2), (3), and (4). For each calculation, a XCO_2 was found for which $\Delta G_{P,T}$ is zero. Two curves were calculated, one by assuming ideal mixing of CO_2 and H_2O (Lewis and Randall rule), so that $\gamma CO_2 = 1$, and another by assuming nonideal mixing, using MRK activity coefficient. The two models fit the data within about 70°C, but the nonideal mixing model provides a closer fit.

Discussion

CO_2 fugacity coefficients

By using MRK fugacity coefficients for CO_2 gas, a decarbonation reaction bracketed at pressures from 2 to 41 kbar has been reduced to 1-bar free energies that plot on a straight line (Fig. 3). The slope of that line, ΔS, is in reasonable agreement with thermochemical data. Of course, as encouraging as this test is, only the consistency of the MRK data set has been demonstrated, not its accuracy. Indeed, apparent deviations have been found, in two studies, between phase boundaries experimentally calibrated and those calculated using MRK functions. These studies, reported only in abstract form, involved CO–CO_2 gas at 13–27 kbar (Woermann *et al.*, 1977) and CO_2 gas at 20–40 kbar (Haselton *et al.*, 1977). Note, however, that one of the test reactions of Haselton *et al.* is the same reaction investigated in this paper. Clarification of these differences must await full publication of the above-mentioned studies.

CO_2 activity coefficients

Activity coefficients for CO_2 in CO_2–H_2O mixtures at 26 kbar can be calculated from the upper curve in Figure 4, using the method described above. These coefficients are shown in Table 1, with uncertainties estimated from possible errors in temperature (the band in Fig. 5) and in pressure. The MRK values, also shown, are near the lower limit of uncertainty of the experimental data.

The actual temperature differences between the MRK curve and the experimental band are less than 40°C (Fig. 5). This difference is considered sufficiently small, at pressures of the mantle, to warrant calculation of the family of decarbonation curves, as a function of XCO_2, to 60 kbar (Fig. 2B). At 60 kbar, MRK γCO_2 ranges from 1.6 ($XCO_2 = 0.1$) to 1.06 ($XCO_2 = 0.8$).

Table 1. Experimental and calculated (MRK) CO_2 activity coefficients in CO_2–H_2O vapor at 26 kbar and approximately 1100°C

x_{CO_2}	0.5	0.3
Experimental	1.40 ± 0.15	1.62 ± 0.13
MRK	1.21	1.47

Petrologic applications

Two reactions delimit the stability of carbonate minerals that coexist with olivine, orthopyroxene, and clinopyroxene. One is the reaction (1) studied here, applicable to the mantle at high pressures, *i.e.* above 44 kbar at 1100°C (Kushiro *et al.*, 1975). At lower pressures, the carbonate mineral in a carbonated peridotite is dolomite rather than magnesite, by the reaction

$$2\ MgSiO_3 + 0.5\ CaMg(CO_3)_2 = 0.5\ CaMgSi_2O_6 + Mg_2SiO_4 + CO_2 \qquad (5)$$

The temperature of reaction (5) at all pressures is about 40°C higher than the temperature of reaction (1), and likewise the vapor composition contours on the divariant surface for reaction (5) are shifted about 40°C higher than the equivalent contours for reaction (1). In essence, then, the surface in Figure 2B denotes the upper stability of a carbonated peridotite at any pressure, to a first approximation. The approximation is improved at lower pressures because the error due to change in reaction (40°C) is offset by the effect of substitution of iron in the reactants and products; Newton and Sharp (1975) calculated this effect to be about 25°C for a typical peridotite composition. At higher pressures the curves shown would be lowered about 25°C by iron substitution. Other elements contained in pyroxenes in natural peridotites (Na, Cr, Al) are unlikely to significantly affect the reactions.

With the above limitations in mind, it should be apparent from Figure 2B that carbonated peridotite is stable over a large *P–T* range even in the presence of H_2O-rich vapor. The principal crystalline phases in such a carbonated peridotite at pressures greater than about 44 kbar (subsolidus) will be oliv + opx + cpx + garnet + magnesite or, at lower pressures, oliv + opx + cpx + garnet (or spinel) + dolomite. [It is possible, by reaction (1) or (5), to carbonate a peridotite composition sufficiently to remove olivine or clinopyroxene; that degree of carbonation requires in excess of 20 weight percent CO_2, however, an unreasonable amount in any model of the mantle.] A CO_2–H_2O vapor phase will coexist with the carbonate minerals unless all the available H_2O is contained in a hydrous phase or, under supersolidus conditions, in a liquid (on the assumption that reduced species such as CO and CH_4 are not present in significant amounts). The possibility that available H_2O *could* be contained in a hydrous phase was considered by Eggler (1978), who concluded that vapor would be present above about 23 kbar, inasmuch as the hydrous phase stable at these pressures, phlogopite, would be present in such small amounts that it would tie up only about 0.02 weight percent H_2O. At lower pressures, an amphibolitic peridotite could contain up to 0.4 weight percent H_2O, and vapor might be absent. At still lower pressures, however, dolomite is not stable (Fig. 2B), and vapor will again coexist with amphibole.

Superposition of geotherms on Figure 2B reveals that although dolomite or magnesite will not be a stable phase of peridotite along a steep oceanic geotherm, a carbonate will be stable at temperatures along a shield geotherm, unless coexisting vapor is exceptionally H_2O-rich. Also shown in Figure 2B is the peridotite solidus applicable to peridotite containing small amounts of CO_2 and H_2O (Eggler, 1977). [For small amounts of volatiles, the vapor composition is buffered by a reaction such as (5) within a zone of invariant vapor composition (ZIVC), and hence the solidus is univariant.] It is apparent that dolomite or magnesite could be a participant phase in the melting of peridotite at pressures greater than about 22 kbar.

Acknowledgments

This study was supported by NSF grants DES 73-00266A01 and EAR 77-15704 (Eggler). The work of Holloway was partially supported by the Geophysical Laboratory through the good offices of Dr. H. S. Yoder, Jr.

The manuscript was reviewed by D. Rumble III, B. O. Mysen, D. M. Kerrick, and H. S. Yoder, Jr.

References

Bell, P. M. and H. K. Mao (1971) Subsolidus reactions of jadeite ($NaAlSiO_6$) and albite ($NaAlSi_3O_8$). *Carnegie Inst. Wash. Year Book, 69,* 168–170.

Clark, S. P. and A. E. Ringwood (1964) Density distribution and constitution of the mantle. *Rev. Geophys., 2,* 35–88.

Eggler, D. H. (1975) Peridotite–carbonate relations in the system $CaO-MgO-SiO_2-CO_2$. *Carnegie Inst. Wash. Year Book, 74,* 468–474.

——(1976) Does CO_2 cause partial melting in the low-velocity layer of the mantle? *Geology, 4,* 69–72.

——(1977) The principle of the Zone of Invariant Vapor Composition: an example in the system $CaO-MgO-SiO_2-CO_2-H_2O$ and implications for the mantle solidus. *Carnegie Inst. Wash. Year Book, 76,* 428–435.

——(1978) Stability of dolomite in a hydrous mantle, with implications for the mantle solidus. *Geology, 6,* 397–400.

——, I. Kushiro and J. R. Holloway (1976) Stability of carbonate minerals in a hydrous mantle. *Carnegie Inst. Wash. Year Book, 75,* 631–636.

——, B. O. Mysen and T. C. Hoering (1974) Gas species in sealed capsules in solid-media, high-pressure apparatus. *Carnegie Inst. Wash. Year Book, 73,* 228–232.

Hariya, Y. and G. C. Kennedy (1968) Equilibrium study of anorthite under high pressure and temperature. *Am. J. Sci., 266,* 193–203.

Haselton, H. T., Jr., W. E. Sharp and R. C. Newton (1977) Decarbonation reactions and derived CO_2 fugacities at high pressures and temperatures (abstr.). *EOS, 58,* 1243.

Holloway, J. R. (1977) Fugacity and activity of molecular species in supercritical fluids. In D. G. Fraser, Ed., *Thermodynamics in Geology,* p. 161–181. D. Reidel Publishing Company, Boston, Massachusetts.

Huang, W. L. and P. J. Wyllie (1975a) Influence of mantle CO_2 in the generation of carbonatites and kimberlites. *Nature, 257,* 297–299.

—— and —— (1975b) Melting relationships in the systems $CaO-CO_2$ and $MgO-CO_2$ to 33 kilobars. *Geochim. Cosmochim. Acta, 40,* 129–132.

Johannes, W. (1969) An experimental investigation of the system $MgO-SiO_2-H_2O-CO_2$. *Am. J. Sci., 267,* 1083–1104.

Kushiro, I., H. Satake and S. Akimoto (1975) Carbonate-silicate reactions at high pressures and possible presence of dolomite and magnesite in the upper mantle. *Earth Planet. Sci. Lett., 28,* 116–120.

Newton, R. C. and W. E. Sharp (1975) Stability of forsterite + CO_2 and its bearing on the role of CO_2 in the mantle. *Earth Planet. Sci. Lett., 26,* 239–244.

Ringwood, A. E. (1966) Mineralogy of the mantle. In P. M. Hurley, Ed., *Advances in Earth Sciences,* p. 357–399. MIT Press, Cambridge, Massachusetts.

Robie, R. A. and D. R. Waldbaum (1968) Thermodynamic properties of minerals and related substances at 298.15°K (25.0°C) and one atmosphere (1.013 bars) pressure and at higher temperatures. *U. S. Geol. Surv. Bull. 1259.*

Wyllie, P. J. and W. L. Huang (1976) Carbonation and melting reactions in the system $CaO-MgO-SiO_2-CO_2$ at mantle pressures with geophysical and petrological applications. *Contrib. Mineral. Petrol., 54,* 79–107.

Woermann, E., B. Knecht, M. Rosenhauer and G. C. Ulmer (1977) The stability of graphite in the system C–O (abstr.). *Extended Abstracts, Second International Kimberlite Conference,* Santa Fe, New Mexico.

Zen, E-an (1972) Gibbs free energy, enthalpy, and entropy of ten rock-forming minerals: calculations, discrepancies, implications. *Am. Mineral., 57,* 524–533.

—— and J. V. Chernosky, Jr. (1976) Correlated free energy values of anthophyllite, brucite, clinochrysotile, enstatite, forsterite, quartz, and talc. *Am. Mineral., 61,* 1156–1166.

Manuscript received, March 31, 1978;
accepted for publication, July 5, 1978.